



## Does “coating resistance” control corrosion?

J.M. Sykes\*, E.P. Whyte, X. Yu, Z. Sharer Sahir<sup>1</sup>

Department of Materials, University of Oxford Parks Rd, Oxford, OX1 3PH, UK



### ARTICLE INFO

#### Article history:

Received 26 December 2015  
Received in revised form 21 March 2016  
Accepted 15 April 2016  
Available online 29 April 2016

#### Keywords:

Resistance inhibition  
Electrochemical impedance spectroscopy  
Coating resistance  
Paint coatings  
Electrode polarisation

### ABSTRACT

Bacon, Smith and Rugg first identified a link between the DC resistance of a coated panel after exposure to salt solution and the performance of the coating in an exposure test. Mayne explained this as “resistance inhibition”. This paper will consider what coating resistance measured by Electrochemical Impedance Spectroscopy (EIS) tells us about factors controlling the corrosion process. It shows that the activation energy for ion conduction does not correspond with that for the corrosion process, suggesting that the paint resistance we measure is not the controlling factor. Furthermore, tests on a model galvanic cell reveal a significant influence of both electrode polarisation and resistance inhibition.

© 2016 Published by Elsevier B.V.

### 1. Introduction

EIS has now become a standard technique for characterisation of organic coatings, and has proved valuable in assessing their performance [1,2]. The impedance behaviour of coated panels can be measured during immersion in a test environment or at intervals during cyclic testing. The coating resistance and other useful information can be extracted by fitting the impedance response across a range of frequencies to a suitable model circuit [1]. A typical model circuit includes the coating resistance and capacitance and components corresponding to the electrochemical behaviour at the metal-coating interface. The capacitance of the coating changes rapidly during first immersion and is often used to measure the rate of water uptake [3]. The coating resistance generally falls over time and is an indication of coating breakdown. Mansfeld [1] identifies the coating resistance as “pore resistance” with conduction by ion transport within pores in the coating. The parameters from the coating-metal interface can in principle quantify the corrosion rate of the underlying metal.

The connection between “coating resistance” and protective performance was identified by Bacon, Smith and Rugg as long ago as 1948 [4]. They carried out DC resistance tests on coated panels over a few weeks of immersion and compared the results with the exposure performance of the same systems. Over 300 samples were tested and it was found that those which performed well out-

doors all showed a high resistance ( $>10^8 \Omega \text{ cm}^2$ ) over the whole period of the laboratory test. With poor coatings, resistance quickly fell by several orders of magnitude. They proposed that “coating resistance” could be used to identify good and bad coatings from laboratory tests.

However, we should recognise that these tests were on coated steel panels and the separate impedances of the coating and the coating-metal interface were not determined. Yet the DC current has to pass through both the resistance of the coating and that of the interface which add together because they are connected in series. If the coating was good and the corrosion rate extremely low, we can infer from the Stern-Geary equation [5] that the polarisation resistance of the interface (inversely proportional to the corrosion rate) must be high and likely to be similar to that of the coating.

Mayne [6] supports the argument that the ionic resistance of a coating is the chief factor providing protection, ruling out transport of oxygen or water as rate-controlling processes, and suggesting a mechanism (“resistance inhibition”) by which the coating resistance greatly reduces the corrosion current. This supposes (based on experimental observations of alkali-filled cathodic blisters separate from the orange rust spots after exposure of painted steel panels to salt solution) that corrosion occurs by an electrochemical mechanism with anode and cathode at different sites beneath the coating. Electrons pass from anode to cathode through the metal, but for current to flow around a complete circuit charge needs to pass, as ions, through the coating at both anode and cathode. Fig. 1 shows a schematic representation of these processes.

Mayne also suggested a way to modify the Evans diagram [7] to include the ohmic potential drop through the coating,  $iR_f$ . This takes account of the fact that with the coating the anode and cath-

\* Corresponding author.

E-mail address: [john.sykes@materials.ox.ac.uk](mailto:john.sykes@materials.ox.ac.uk) (J.M. Sykes).

<sup>1</sup> Present address: UTM-MPRC, Institute for Oil & Gas, Universiti Teknologi Malaysia, Skudai, 81310 Johor, Malaysia.

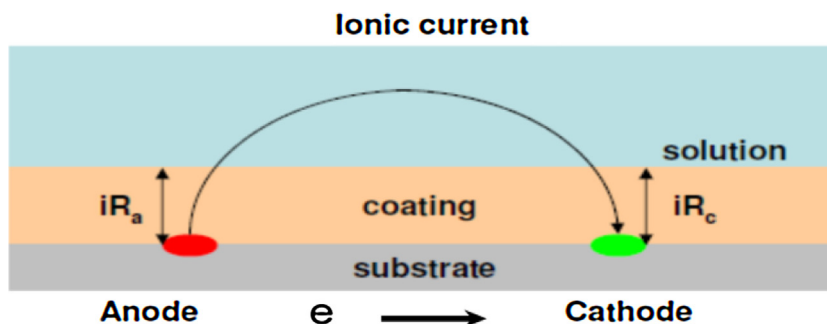


Fig. 1. A schematic representation of a corrosion cell beneath an organic coating to illustrate the operation of resistance inhibition.

ode are no longer at the same potential, because a potential drop is needed to drive the corrosion current through the paint. The film resistance,  $R_f$ , consists of two parts,  $R_a$ , the resistance of the current pathway through the coating above the anode (or anodes) and  $R_c$ , that above the cathodes. The separate ohmic potential drops can be indicated on the diagram, with the potential measured by a reference electrode in the test solution lying below that for the cathode (if a reference electrode were to be placed below the paint) and above that for the anode. The position of this potential will depend upon the relative magnitudes of  $R_a$  and  $R_c$ , so that if  $R_a$  falls as corrosion develops the measured potential of the panel falls, even if the potentials of the anode and cathode remain the same.

In Fig. 2 current has been plotted on a logarithmic scale, to accord with Tafel behaviour, rather than the linear scale used by Mayne.

This model will not fit all circumstances, for instance Kendig [8] observed with a thin coating of polybutadiene on steel that cathodic disbonding by cathodic alkali took place around dark rust spots, showing that a direct ionic pathway existed between anode and cathode. A similar situation exists with neutral blisters where anode and cathode co-exist within the blister. Doherty demonstrated by scanning Kelvin probe (SKP) and scanning acoustic microscopy (SAM) that anodic blisters could develop alongside, and connected to, cathodic blisters then as rust precipitated out became cathodes that triggered the development of fresh anodic blisters [9]. In these situations the cell current has no need to pass through the paint.

What we wish to highlight with Mayne's model (see Fig. 1) is that in the path for the corrosion current  $R_a$  and  $R_c$  are connected

together in series, so if one is much bigger than the other then the larger one controls the corrosion rate, yet when we measure the resistance between the metal and the solution (as we do with EIS or similar methods) then the resistances are connected in parallel and the smaller of the two will control the measured value. The implication is that we can't directly measure the parameter we really need to know.

The aim of this paper is to develop this argument and see if this difficulty is real. It will bring together recent published research results from Oxford students [10–14] and put them into context. I will not try in this short paper to bring together the many other pieces of supporting (or opposing) evidence that can be culled from the work of other researchers

## 2. Methods and materials

The first part of this work [10] was carried out to investigate the behaviour of an organic coating on galvanised steel and better understand how the galvanic cell established when a small area of zinc is removed by damage (or at a cut edge) would operate if anode and cathode were both covered by a polymeric coating. Is the current large enough to provide sacrificial protection? To understand this situation separate electrodes of mild steel (Q-panel) and pure zinc (Advent Research Materials Ltd.) were mounted side-by-side in cold-setting resin (Lecoset), ground flat, and coated with a thin ( $d_{ft} = 45 \mu\text{m}$ ) film of poly(vinyl butyral) using a spreader bar. Full details have been published elsewhere [10]. When the sample was immersed face down in 1% by weight NaCl solution this arrange-

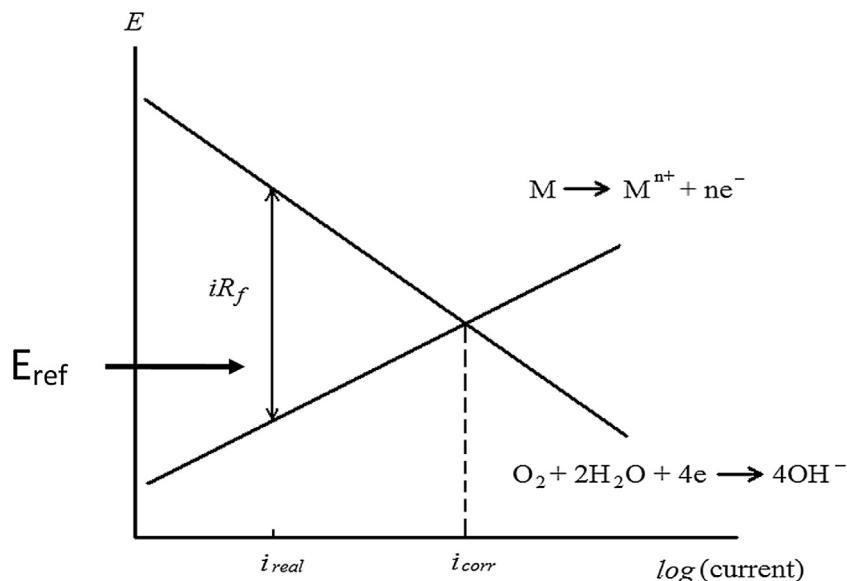


Fig. 2. Mayne's modification of an Evans diagram to allow for coating resistance.

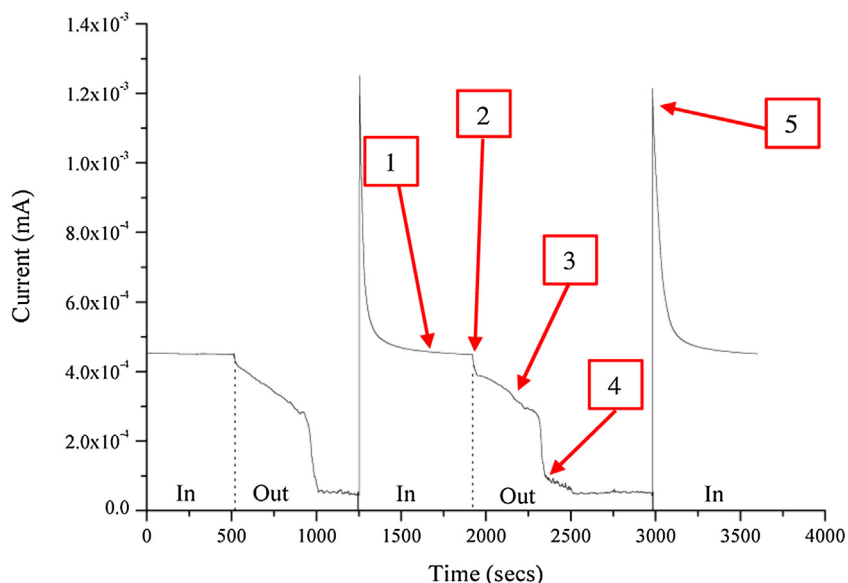


Fig. 3. Current changes in a zinc-steel bi-electrode when switched between in and out of the test solution (after days immersion) [10].

ment allowed the galvanic current to be measured continuously with anode and cathode connected externally via a zero-resistance ammeter (Gill AC potentiostat), and for the impedance of the whole cell (with electrodes connected), or of the separate electrodes, to be measured using a saturated calomel electrode (SCE) as reference and a small platinised titanium counter electrode immersed in the working solution. Impedance was measured from 0.1 Hz – 1 kHz (with 25 data points), using an amplitude of 20 mV. Impedance measurements were always made under potentiostatic control at the potential of the galvanic couple, so that during the separate tests a DC current passed as if the two electrodes were still connected to each other. A further set of tests was conducted [11,12] with the same type of cell using either a similar steel-zinc bi-electrode or another with two steel electrodes where a small droplet of 3% NaCl had been placed on one of the electrodes and allowed to dry (with consequent development of orange rust) before the coating was applied. In this work unpigmented coatings of PVB, a vinyl and a 2-pack epoxy were employed. Full details are in the papers.

In some cases, to quantify the behaviour of the system, polarisation curves for the two electrodes were plotted using a “potentiostatic pulse” method (usually at the end of a series of EIS tests). This should in principle allow the film resistance and steady current at each potential to be determined simultaneously [15]. In practice it proved more reliable to step the potential from the open circuit value and record the current after 2 min as the steady value (for consistency), but to correct the applied potential in the polarisation curve for the ohmic potential drop in the coating using the coating resistance determined from EIS. Thus Mayne’s diagram was constructed by plotting anode and cathode curves onto  $E/\log i$  axes with the  $iR_f$  arrow drawn at the *known* value of couple current. Thus Mayne’s construction can be validated and the relative roles of resistance inhibition and electrode polarisation determined.

In a parallel study [13,14] mild steel panels were coated with epoxy or epoxy-phenolic coatings and immersion tested in hot NaCl solutions. EIS measurements were made periodically (as above, but at the free corrosion potential) across a range of temperatures. The results were fitted to a model circuit using a non-linear least-squares fitting program (ZsimpWin) and where two distinct time constants could be identified the values of the coating resistance and charge transfer resistance were obtained by least-squares fitting of the model circuit, then plotted as  $\log R$  vs.  $1/T$  (Arrhenius plots) to determine activation energies for the processes involved.

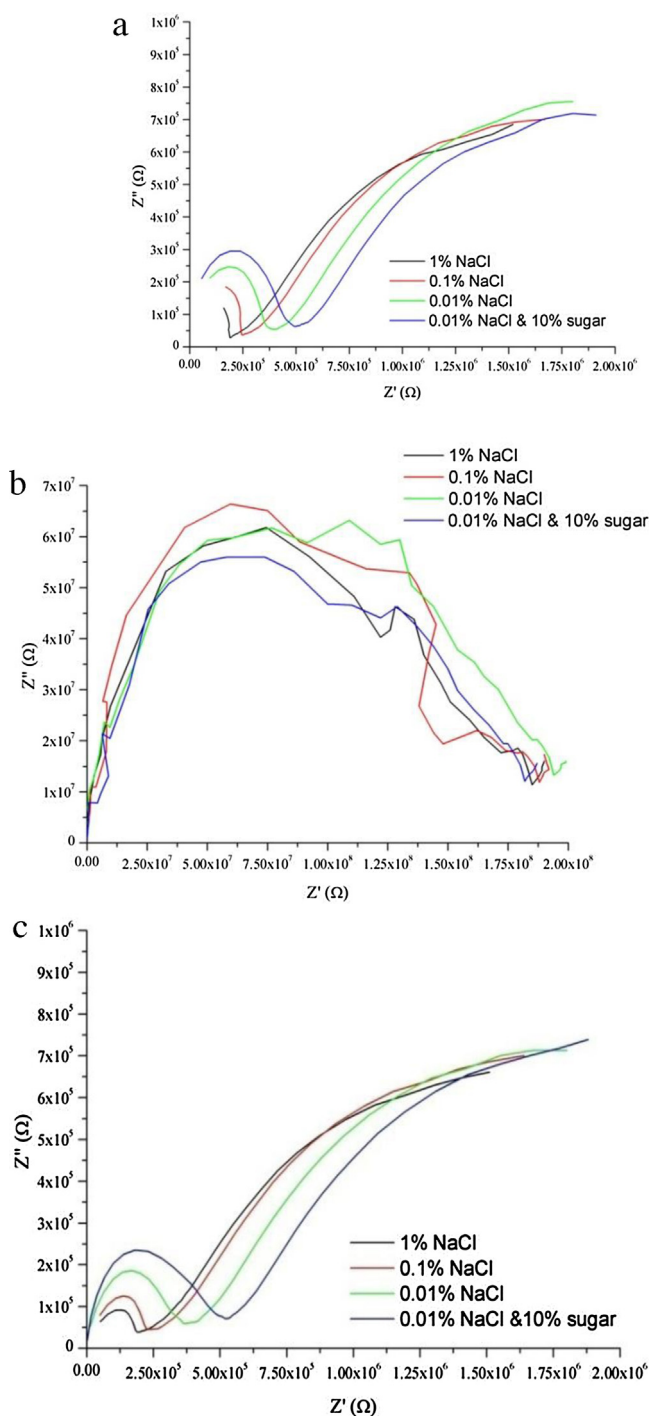
### 3. Results

Fig. 3 shows a ZRA current trace after almost 13 days of immersion. In this test the sample has been removed from the solution and dried with tissue in order to determine whether current can pass from anode to cathode along the paint-metal interface or only flows through the coating and solution as in Mayne’s model. Although a small residual current does flow after removal from solution (labelled 4), it is clear that the almost all of the current (labelled 1) flows via the solution while the sample is immersed. The current traces show large spikes when the sample is re-immersed (labelled 5) which will be argued later to be an indication of polarisation of the electrode process (but were previously linked with water loss during the dry period [10]).

Fig. 4. shows separate Nyquist plots for the steel and the zinc and the result for the coupled pair, all taken on the 13 day. In this instance the zinc shows two semi circles, whereas the steel gives only one, but the impedance of the coated steel is very much greater than that of the zinc. Thus if the pair is coupled the impedance response is virtually identical to that of the zinc, because the low impedance of the zinc + coating short circuits that of the steel + coating. These preliminary experiments confirm that the highest resistance in the current pathway for a zinc-steel couple cannot here be determined from EIS on the coupled electrodes. The same would be true for a piece of coated galvanised steel with the underlying steel exposed.

The plots in Fig. 4 show results for immersion in solutions with different salt concentrations – used to ascertain the mode of conduction in the coating. The zinc sample shows that coating resistance (from the high frequency semi-circle) increased as the salt solution was diluted: D type behaviour [16] as expected for this coating, but the steel showed little change. It is of particular interest to note that when sucrose was added to the most dilute salt solution (which will lower water activity), there is a further increase in resistance, showing that for D films resistance is influenced by water activity, the controlling factor with I films, as well as ion concentration.

Fig. 5 shows similar results for a different zinc-iron couple coated with 40  $\mu\text{m}$  of the vinyl coating after 13 days exposure to salt solution [11]. Here the impedance of the steel (a) is still high but much smaller than the zinc (b). Both show a distinct high-frequency semi-circle arising from the coating resistance but that on the steel



**Fig. 4.** Nyquist plots showing EIS results for 45  $\mu\text{m}$  thick poly(vinyl butyral) coatings on (a) zinc, (b) steel and (c) coupled zinc-steel during exposure to the solutions indicated [10].

is clearly much smaller. When we examine the plot for the couple (c) we can see that it closely resembles that for steel and is not influenced by simultaneous connection to the zinc (remembering that the potential has been held the same for both).

For the clean steel-rusty steel couple with an epoxy coating, the rusty steel became the anode, but for the first few hours exhibited an impedance  $>10^9 \Omega$ ; however after 24 h the impedance for the rusty steel was clearly much smaller than the clean steel, and remained so as the test progressed (Fig. 6(a) and (b)). When the two electrodes are measured coupled together (c) the plot is the same

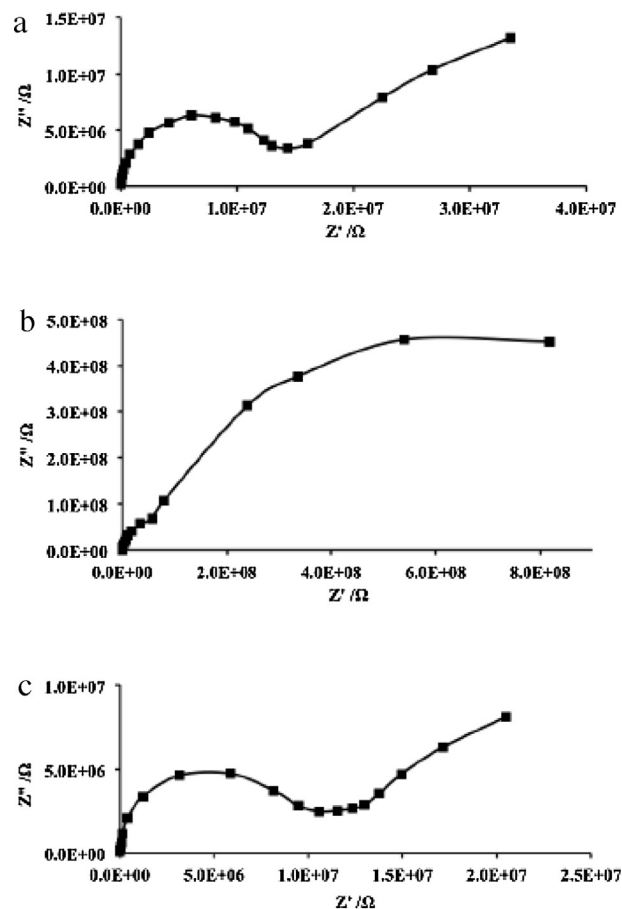


**Fig. 5.** Nyquist plots showing EIS results for (a) steel, (b) zinc and (c) coupled zinc+steel coated with 40  $\mu\text{m}$  of clear vinyl exposed to 1% NaCl after 13 days exposure.

as the rusty electrode, and the behaviour of the clean steel which is expected to control the corrosion rate, because of its much higher resistance, cannot be detected.

When potential pulse tests were carried out after 7 days exposure and plotted with the potential values corrected for ohmic potential drop in the coating so as to show the true polarisation behaviour, reasonable Tafel lines were fitted (Fig. 7), though care was needed to choose the correct film resistance values [13]. The arrow has been drawn at a couple current of 19 nA and the ohmic potential drop is found to be 145 mV, which agrees quite well with the calculated value [ $=i(R_a + R_c)$ ].

At this point both reactions are polarised significantly, but the ohmic potential drop also produces a sizeable reduction in current. Similar results were obtained with Zn-steel and Cu-steel couples.

The tests at elevated temperature on steel panels coated with polyamide cured epoxy and epoxy-phenolic coatings showed a rapid fall in impedance over a few days, yet the same coatings sustained a much higher resistance when tested at room temperature over periods of weeks typical of “good” coatings.

When samples tested at 50  $^\circ\text{C}$  were allowed to cool and EIS measurements were made across a range of lower temperatures, then impedance significantly increased. Fig. 8 shows a result for a polyamide cured epoxy coating 75  $\mu\text{m}$  thick after 3 days exposure to 3% NaCl at 50  $^\circ\text{C}$ . Curves such as this, where two distinct semi-circles can be seen, were selected to obtain independent measurements of coating resistance and charge-transfer resistance.

By fitting a model circuit (Fig. 9) the resistance of the coating and the charge-transfer resistance of the corrosion reactions at the interface were determined.

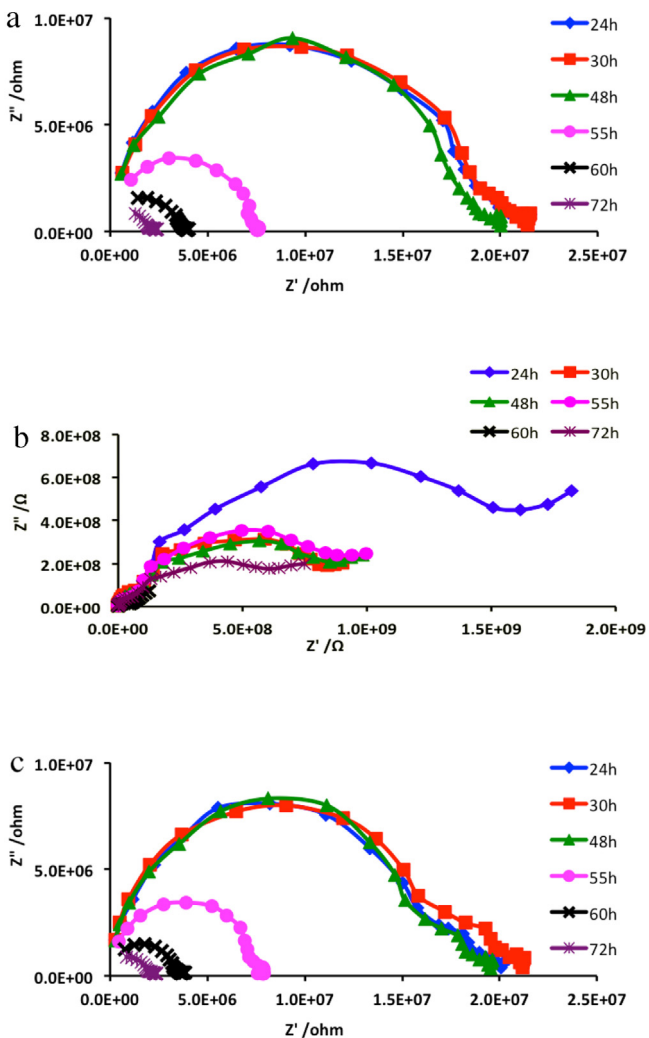


Fig. 6. EIS results for a clean steel-rusty steel couple coated with a 86 μm epoxy coating. ((a) rusty steel, (b) clean steel, (c) clean and rusty steel coupled together, after exposure to NaCl solution for the times indicated).

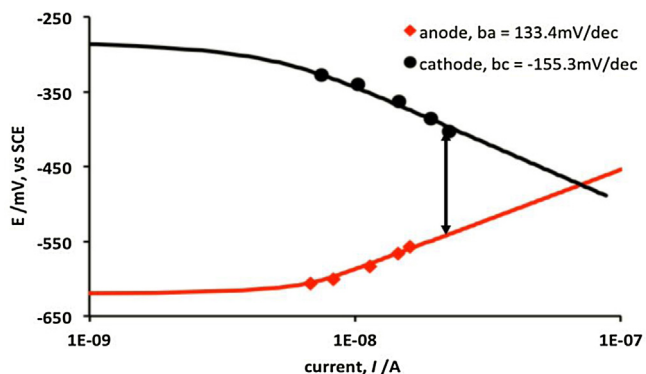


Fig. 7. Evans diagram for clean steel-rusty steel couple with logarithmic current axis, showing Tafel slopes and  $iR$  drop in coating at couple current [13].

From these resistance values Arrhenius plots ( $\log R$  vs  $1/T$ ) were made for this coating and the epoxy phenolic to determine activation energies for the rate-controlling processes. In Figs. 10 and 11 a good fit to the Arrhenius equation can be seen for both the coating resistance and the charge transfer-resistance that depends upon corrosion rate. It is evident that for both coatings the process that determines  $R_{ct}$  and controls corrosion has a higher activation

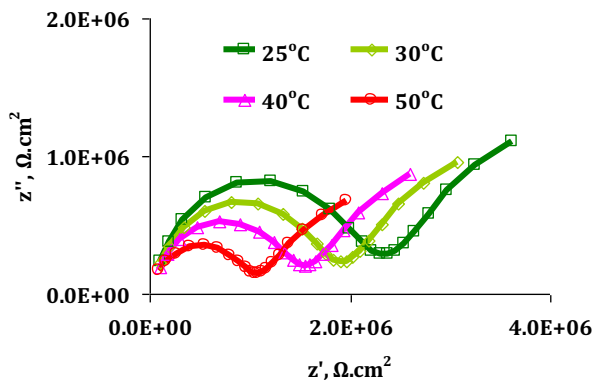


Fig. 8. Nyquist plots for a polyamide cured epoxy coating 75 μm thick after 3 days exposure to 3% NaCl at 50 °C tested at the temperatures indicated.

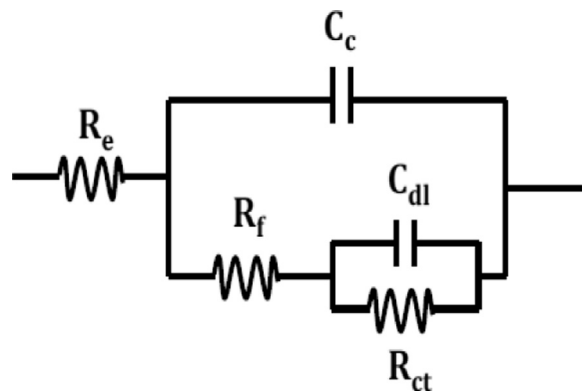


Fig. 9. Model circuit:  $R_f$  = film resistance,  $C_c$  = coating capacitance,  $C_{dl}$  = double layer capacitance,  $R_p$  = charge transfer (or polarisation) resistance.

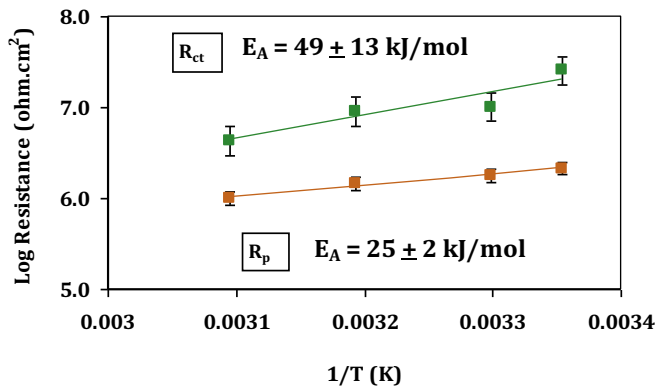


Fig. 10. Arrhenius plots for  $R_{ct}$  and  $R_p$  for a polyamide cured epoxy coating 75 μm thick after 3 days exposure to 3% NaCl at 50 °C [15].

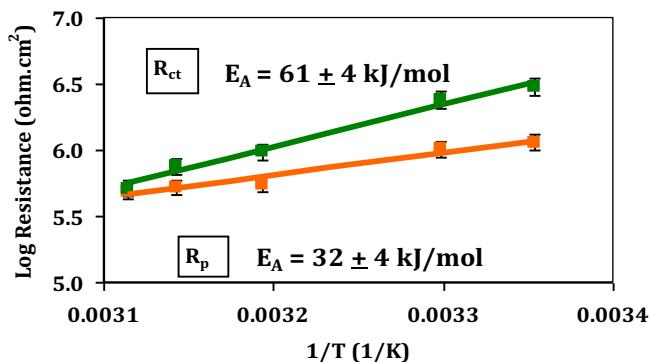


Fig. 11. Arrhenius plots for  $R_{ct}$  and  $R_p$  for an epoxy-phenolic coating 150 μm thick after 30 days exposure to 3% NaCl at 50 °C [15].



energy that for ionic conduction in the coating which determines  $R_f$ . The activation energies for ionic conduction are similar to those obtained by Mayne for D type samples [17]. Panels of this size would be expected to include D regions in the coating that would control the overall resistance, because of their lower resistance.

#### 4. Conclusions

The EIS tests on bi-electrodes have made it quite clear that in many cases the measured impedance of a coated panel will correspond to whichever electrode (anode or cathode) provides the easiest current path and that if the resistance inhibition model for protection holds for those systems the high-resistance pathway which controls the corrosion current is not measurable. The good agreement between film resistance and performance often found in practice may come about because in a good coating both are high.

The tests on coated panels at elevated temperature show that the temperature dependence of the measured impedance does not match that of the corrosion process. This shows that the coating resistance we measure cannot be controlling the corrosion process. However it remains possible that if the higher part of the total resistance between anode and cathode, at either cathode or anode, (which cannot be measured) is in control, then the activation energy for ion transport for that part of the coating could be higher and determine the activation energy for the corrosion process. Higher activation energies have been found for intact free films of paint [15,17].

The potential pulse tests on bi-electrodes have produced examples of “Mayne diagrams” in which the electrode behaviour is credible and the ohmic potential drop that produces resistance inhibition can be measured experimentally. In some cases polarisation of both electrodes is clearly present, so that the corrosion process is under mixed control.

#### Acknowledgements

We are grateful to Shell International and Akzo Nobel for financial support, materials and helpful discussions, to EPSRC and Corus

for a CASE studentship for EPW, to the Ministry of Higher Education of Malaysia and the University Technology of Malaysia for a scholarship for ZSS and to the K.C. Wong Foundation and the University of Oxford for a graduate scholarship for YX.

#### References

- [1] F. Mansfeld, Use of electrochemical impedance spectroscopy for the study of corrosion protection by polymer coatings, *J. Appl. Electrochem.* 25 (1995) 187.
- [2] M. Kendig, F. Mansfeld, S. Tsai, Determination of the long-term corrosion behaviour of coated steel with A.C. impedance measurements, *Corros. Sci.* 23 (1983) 317.
- [3] D.M. Brasher, A.H. Kingsbury, Electrochemical measurements in the study of immersed paint coatings on metal: i Comparison between capacitance and gravimetric methods of estimating water uptake, *J. Appl. Chem.* 4 (1954) 62.
- [4] R.C. Bacon, J.J. Smith, F.M. Rugg, Electrolytic resistance in evaluating protective merit of coatings on metals, *J. Ind. Eng. Chem.* 40 (1948) 161.
- [5] M. Stern, A.L. Geary, Electrochemical polarization: i A theoretical analysis of the shape of polarisation curves, *J. Electrochem. Soc.* 104 (1957) 56.
- [6] J.E.O. Mayne, Electrochemical behaviour of paint films in seawater, *Chem. Ind.* (1951) 293.
- [7] J.E.O. Mayne, Mechanism of the corrosion protection of iron and steel by paint, *Anti-Corros. Methods Mater.* 20 (1973) 3–8.
- [8] H. Leidheiser Jr., M. Kendig, The mechanism of corrosion of polybutadiene-coated steel in aerated sodium chloride, *Corrosion* 32 (1976) 69.
- [9] M. Doherty, J.M. Sykes, Micro-cells beneath organic lacquers: a study using scanning Kelvin probe and scanning acoustic microscopy, *Corros. Sci.* 46 (2004) 1265.
- [10] E.P. Whyte, J.M. Sykes, Behaviour of a zinc-iron bimetallic couple coated with polyvinyl butyral lacquer during intermittent exposure to salt solution, *Corr. Sci.* 49 (2007) 3361.
- [11] J.M. Sykes, Y. Xu, Electrochemical studies of galvanic action beneath organic coatings, *Prog. Org. Coat.* 74 (2012) 320.
- [12] Y. Xu, J.M. Sykes, The influence of electrode polarization on corrosion beneath paint, *Prog. Org. Coat.* 74 (2012) 549.
- [13] P.C. Pistorius, Electrochemical testing of intact organic coatings, *Proc. 14th Int. Corros. Congress* (Cape Town, S. A.) published on CD-ROM, 1999.
- [14] Z. Sharer Sahir, J.M. Sykes, Insights into the protection mechanisms of organic coatings from thermal testing with EIS, *Prog. Org. Coat.* 74 (2012) 405.
- [15] Z. Sharer Sahir, Effect of temperature on the impedance response of coated metals, *Prog. Org. Coat.* 77 (2014) 2039.
- [16] J.E.O. Mayne, J.D. Scantlebury, Ionic conduction in polymer films II Inhomogeneous structure of varnish films, *Br. Polym. J.* 2 (1970) 240.
- [17] J.E.O. Mayne, D.J. Mills, Structural changes in polymer films. Part 1: the influence of the transition temperature on the electrolyte resistance and water uptake, *J. Oil Col. Chem. Assn.* 65 (1982) 139.